Chemical Science

ROYAL SOCIETY OF CHEMISTRY

EDGE ARTICLE

View Article Online
View Journal | View Issue

Cite this: *Chem. Sci.*, 2025, **16**, 11375

All publication charges for this article have been paid for by the Royal Society of Chemistry

Received 22nd April 2025
Accepted 16th May 2025

DOI: 10.1039/d5sc02953h

rsc.li/chemical-science

Bio-inspired total synthesis of daphnepapytone A†

Joan Pereira, [a] Nicolas Casaretto, [b] Gilles Frison [c] and Bastien Nay *[a]

Daphnepapytone A (**1**) is an unprecedented guaiane-derived sesquiterpene characterized by a bridged and highly substituted cyclobutane. We describe its total synthesis through a bio-inspired sequence of skeleton construction and late-stage oxidation. After the Eschenmoser–Tanabe fragmentation of (*R*)-carvone epoxide, the allenylation of the resulting aldehyde was followed by an allenic Pauson–Khand reaction with distal regioselectivity in the presence of $[Rh(CO)_2Cl]_2$ to give the guaiane skeleton. Oleodaphnone (**3**) was identified as a key intermediate of this strategy and was engaged in a biomimetic [2 + 2]-photocycloaddition, leading to the bridged cyclobutane of the title compound. Finally, a late-stage C–H oxidation chemoselectively released a triketone intermediate (**15**), which was reduced in a remarkably chemo- and stereoselective manner to furnish target compound **1**. During this work, complex rearrangements of the bridged skeleton were observed. Beside the total synthesis of daphnepapytone A, this paper also describes the total synthesis of three guaiane natural products (oleodaphnone, diarthroncha C, daphnenicillata W), one of them being structurally revised.

Introduction

Since Komppa's pioneering synthesis of camphor in 1903,[1] bridged terpenes have always been considered as challenging targets in total synthesis (Fig. 1a). In particular, sesquiterpenes offer an infinite structural playground for this purpose, often with a strong medicinal importance. Longifolene, one of the flavouring molecules of the lapsang souchong tea, is a famous representative example of synthetic target that inspired various strategies, like those of Corey[2] or Oppolzer.[3] More recently, the enantioselective total synthesis of artatrovirenol A, a potentially anticancer guaiane-derived compound with a rare and complex caged structure, was independently reported by Zhu,[4] and by Xie and She,[5] the last one involving a biomimetic intramolecular Diels–Alder reaction to install the bridged system. Beside complex carbocyclic skeletons, the degree of functionalization of terpenes adds a significant level of synthetic complexity, especially in terms of oxidation levels. The development of late-stage oxidative C–H functionalization represents a breakthrough in total synthesis, allowing circumvention of long multistep sequences.[6–15] This strategy was referred to as a bio-inspired "two-phase" approach by Baran,[16–19] involving the "cyclase phase" aimed at skeleton construction and the "oxidase phase" aimed at skeleton functionalization (Fig. 1b). Although it is straightforward and applicable to synthetic targets as complex as taxol,[19] this strategy is characterized by a significant challenge related to reactivity and selectivity issues during the oxidase phase.

Daphnepapytone A (**1**, Fig. 1a) is a guaiane-derived sesquiterpene isolated in 2022 by Zhao, Dai and co-workers from *Daphne papyracea* ("Xuehuagou"), an ornamental plant also

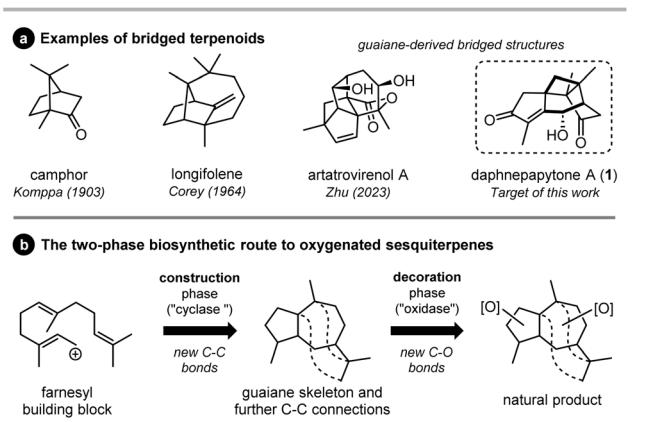

Fig. 1 (a) Selected examples of bridged terpenoids (the authors of the first synthesis are italicized), and (b) general two-phase biosynthetic origin of oxygenated sesquiterpenes as an inspiration for total synthesis.

[a]*Laboratoire de Synthèse Organique, Ecole Polytechnique, ENSTA Paris, CNRS, Institut Polytechnique de Paris, Route de Saclay, F-91128 Palaiseau Cedex, France. E-mail: bastien.nay@polytechnique.edu*

[b]*Laboratoire de Chimie Moléculaire, Ecole Polytechnique, ENSTA Paris, CNRS, Institut Polytechnique de Paris, Route de Saclay, F-91128 Palaiseau Cedex, France*

[c]*Laboratoire de Chimie Théorique, Sorbonne Université, CNRS, F-75005 Paris, France*

† Electronic supplementary information (ESI) available: Fig. S1–S6, Tables S1–S23, detailed experimental procedures, copies of NMR and HRMS spectra, computational details and crystallographic data (.pdf). Cartesian coordinates for computational studies are provided in a separated file (.xyz). CCDC 2418568 (**15**), 2418571 (**1**), 2418579 (**3**), 2419407 (**2**), 2419408 (**13**), 2419409 (**9b**), 2423044 (**19**) and 2428644 (**14**). For ESI and crystallographic data in CIF or other electronic format see DOI: https://doi.org/10.1039/d5sc02953h

used to treat diabetes and inflammatory diseases in Southern China.[20] This oxygenated cage structure holds a rare bridged and highly substituted cyclobutane ring. It thus constitutes an unprecedented target for total synthesis, which is further justified by its α-glycosidase inhibitory properties and a limited extraction yield (5.3 mg out of 12.3 kg of air-dried plant stems). Indeed, considering this challenging synthetic target, a straightforward synthetic route is awaited if we are to use **1** as a lead compound to design new natural product-based antidiabetic treatments.

To synthesize daphnepapytone A, we envisaged a bio-inspired strategy[21–25] combining a highly efficient skeleton construction from (*R*)-carvone and a challenging late-stage C–H oxidation performed on bridged intermediate **2** (Scheme 1). Compound **2** was expected to be formed in a biomimetic manner from the [2 + 2] cycloaddition of oleodaphnone **3**. This HIV-targeting guaiane sesquiterpene[26] could be the product of an allenic Pauson–Khand reaction (APKR) with a distal regioselectivity permitted by Rh(I)-catalysis.[27,28] Finally, allene intermediate **4** would be available from the allenylation of aldehyde **5**, a product of the Eschenmoser–Tanabe fragmentation of carvone (**6**) epoxide.[29,30] Importantly, while we were submitting this work for publication, an elegant alternative to the APKR was disclosed by Stoltz and co-workers through the Pauson–Khand reaction of a methylidenecyclobutane intermediate.[31,32] This approach was consecutive to a limited success in the biomimetic [2 + 2] cycloaddition.

Results and discussion

To start this synthetic sequence, (*R*)-carvone (**6**) was readily epoxidized in presence of H_2O_2 under basic (NaOH) assistance (Scheme 2). The Eschenmoser–Tanabe fragmentation of the resulting epoxycarvone was conducted in presence of tosylhydrazide in a CH_2Cl_2/AcOH mixture, giving the branched 5-heptynal (**5**) in 43% yield on a decagram scale.[33] The efficient In(0)-promoted allenylation of aldehyde **5** in presence of 2-butynyl bromide[34] afforded a diastereomeric mixture of *gem*-disubstituted allenols **7a** and **7b** ($dr^{4S/4R}$ = 1 : 1.5, partially separable). Noteworthily, the diastereoselective synthesis of allenol **7a** and **7b** was also successfully achieved in presence of (2-butynyl)pinacolborane and chiral phosphoric acids (*R*)- and (*S*)-TRIP (5 mol%),[35] respectively, paving the way to a stereoselective access to **10** and **11**. Alternatively, the diastereomeric mixture of allenols could be oxidized in presence of Dess–Martin periodinane (DMP), furnishing ketone **4** (Scheme 1). This volatile ketone, however, turned out to be unreactive towards the next APKR step (not shown).

After TBS-protection of the secondary alcohols, the Pauson–Khand reaction was envisaged on intermediates **8a** and **8b**, and directly on the diastereomeric mixture (Scheme 2, step 6). It is known that the APKR faces a regioselectivity issue due to the two reactive, distal or proximal alkenes on allenes, depending on the catalytic system and the substitution pattern of the allene.[27,28] Brummond[38–43] and Mukai[44–47] previously showed

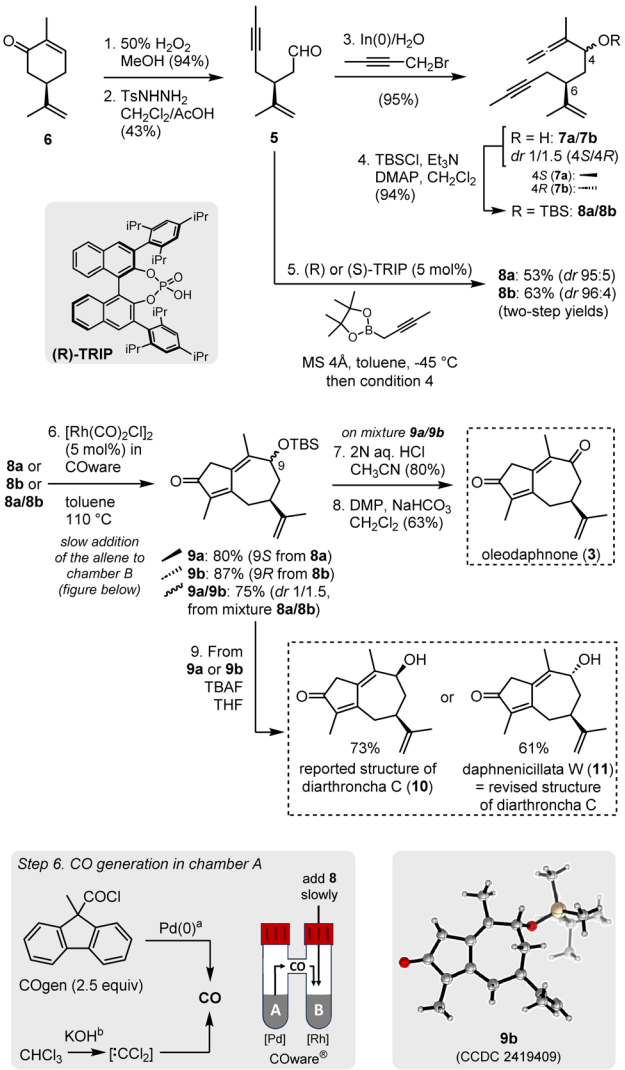

Scheme 2 Total synthesis of oleodaphnone (**3**), diarthroncha C (**10**, structure as reported in the literature), and daphnenicillata W (**11**), through an APKR performed in COware®. Notes: (a) COgen (2.5 equiv.), $PdCl_2$(cod) (10 mol%), [(*t*-Bu)$_3$PH]BF_4 (10 mol%), MeN(Cy)$_2$ (4.0 equiv.), toluene (0.02 M);[36] (b) KOH (30 equiv.), $CHCl_3$ (10 equiv.), toluene (0.05 M).[37] Note: ORTEP structure of **9b** at 50% probability level (CCDC number: 2419409).‡[1]

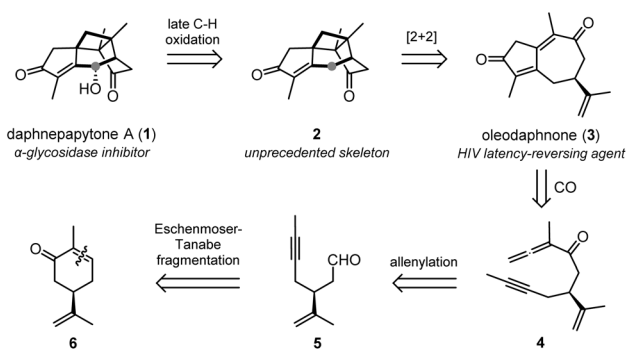

Scheme 1 Retrosynthetic analysis of daphnepapytone A (**1**) through oleodaphnone (**3**).

that a Rh(I)-based catalytic system exclusively results in distal selectivity. To perform this reaction, a Skrydstrup's two-chamber COware® system was used, with CO being safely generated from 9-methyl-9*H*-fluorene-9-carbonyl chloride (COgen) under Pd-catalysis in chamber A (Scheme 2).[36] Thus, the APKR of substrates **8a** and **8b** (added slowly to chamber B)[43] in presence of $[Rh(CO)_2Cl]_2$ (5 mol%) exclusively afforded the 5/7-fused TBS-protected products **9a** and **9b** possessing a guaiane skeleton. The relative stereochemistry of these compounds was deduced from the X-ray crystallographic structure of **9b** (CCDC 2419409). During the optimisation (see Tables S1–S3†), while isomer **8a** gave cleaner and faster reactions, isomer **8b** provided more by-products on similar reaction times, supposedly formed from intermolecular processes.[43] This problem was solved by increasing the addition time of substrate **8b** onto the catalytic system. Furthermore, the APKR on the diastereomeric mixture **8a**/**8b** could be achieved in a 75% yield after an addition time of 20 h on a 1.87 mmol scale. Finally, the catalyst $[Rh(CO)(dppp)_2]Cl$ tested on **8b** gave a lower yield (54%) than $[Rh(CO)_2Cl]_2$, while Pauson–Khand reagents like $Mo(CO)_6$ or $Co_2(CO)_8$ led to degradation or no reaction. To improve the atom-economy and reduce the cost of this two-chamber process, CO was also generated from the reaction of $CHCl_3$ with KOH in chamber A,[37,48] yet with a drop of the APKR yield (55% for mixture **9a**/**9b**).

The deprotection of the diastereomeric mixture **9a**/**9b** under acidic condition (aqueous HCl, CH_3CN), followed by the oxidation of the secondary alcohol with Dess–Martin periodinane (DMP), in 50% yield over two steps, completed the first total synthesis of pale green compound oleodaphnone (**3**, see Table S4† for NMR data comparison with the literature). Alternatively, since this acidic condition was found to induce epimerization of the C-9 stereocenter, the deprotection of pure diastereoisomers **9a** and **9b** in presence of tetrabutylammonium fluoride (TBAF) afforded the two natural products diarthroncha C (**10**, structure shown as reported)[49] and daphnenicillata W (**11**),[50] in 73% and 61% yields, respectively. While the NMR data of **11** matched those of natural daphnenicillata W[50] in $CDCl_3$ (Table S6†), significant deviations were observed for **10** compared to those of natural diarthroncha C[49] in DMSO-d_6 (Table S5†). Fortunately, we also recorded the NMR spectra of **11** in DMSO-d_6, and observed striking similarities with the NMR data of natural diarthroncha C (Table S7†). Consequently, we propose to revise the reported stereochemistry of diarthroncha C as structure **11**. In other words, diarthroncha C and daphnenicillata W are the same compound **11**.

Interestingly, the X-ray crystallographic structure of **3** (CCDC 2418579, Scheme 3) showed an equimolar distribution of two conformers in the crystal, either with a pseudo-equatorial or a pseudo-axial orientation of the isopropenyl group (see also Fig. S1†). The proximity of the isopropenyl olefin with that of the cycloheptenone ring (distance < 4 Å) was observed on the pseudo-axial conformer, supporting the feasibility of the photochemical enone–alkene [2 + 2] cycloaddition.[51] To finally elaborate the carbocyclic skeleton of daphnepapytone A,

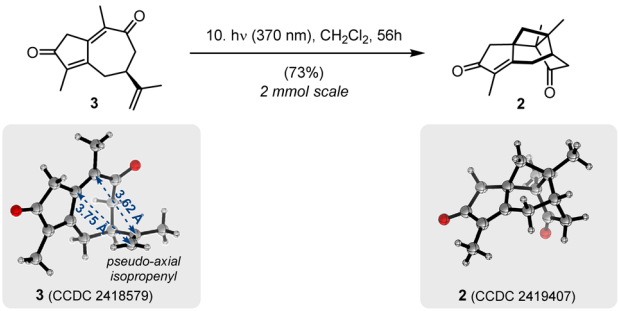

Scheme 3 Biomimetic [2 + 2] cycloaddition of **3**. Note: ORTEP structures at 50% probability level (CCDC numbers for **2**: 2419407; **3**: 2418579).‡

a solution of oleodaphnone **3** in CH_2Cl_2 was irradiated at 370 nm (Kessil lamp), giving the bridged cyclobutane intermediate **2** in 73% yield (Scheme 3, and Fig. S2a† for key NMR correlations). This structure was confirmed by X-ray crystallography (CCDC 2419407). It seems reasonable to suggest that this [2 + 2] cycloaddition is "biomimetic" in the sense that it could occur in the *Daphne* plant under the sunlight. To test this hypothesis—since Paris weather in 2024 did not allow us to copy Ciamician's rooftop condition used in 1908 to photocyclize carvone[52]—a sample of **3** in $CDCl_3$ was treated under white light (LED). NMR monitoring confirmed the formation of **2**, yet in low yield (10%) and with marked degradation after 18 days (Fig. S3†).

Finally, we turned our attention to the late-stage oxidative functionalization of **2**, targeting the γ-position (C-6) of the remaining enone (Scheme 4). This transformation had to be regioselective and stereoselective to install the secondary alcohol of daphnepapytone A (**1**). The reactivity of caged intermediate **2** was thus investigated under various conditions. Compound **2** turned out to be neither reactive under Riley oxidation condition in presence of SeO_2, nor toward the formation of a dienol silyl ether targeting a vinylogous Rubottom reaction toward **1** (Table S8†). While photooxygenation attempts[53] in presence of singlet oxygen led to degradation (see Table S9† for other attempts), the application of autooxidation conditions in presence of *t*BuOK under air (route a) provided a new, rearranged but non-oxidized structure (**13**, see Fig. S2b† for key NMR correlations) in 40% yield (or 67% when performed under argon). The 1,2-migration of C-10, with concomitant ring expansion of the cyclobutane ring, was supposed to proceed through a base-promoted retro-Michael addition followed by a new Michael addition on C-5 of the cyclopentadienone intermediate **12**. X-ray crystallographic analysis confirmed structure **13** (CCDC 2419408).

Most interestingly, based on Newhouse's precedent, the application of the 2-hydroxy-2-methyl-butanoic acid chromium complex Cr(v) (route b) not only afforded 6-*epi*-daphnepapytone A (***epi*-1**) as a major compound (28% yield, or 46% b.r.s.m.), but also the rearranged triketone **14** (12%), a substantial amount of remaining starting material (40%) and traces of ketone **15**. Despite its appealing character confirming the possibility to

‡ X-ray and model structures were generated with CYLview20, C. Y. Legault, Université de Sherbrooke, 2020 (https://www.cylview.org).

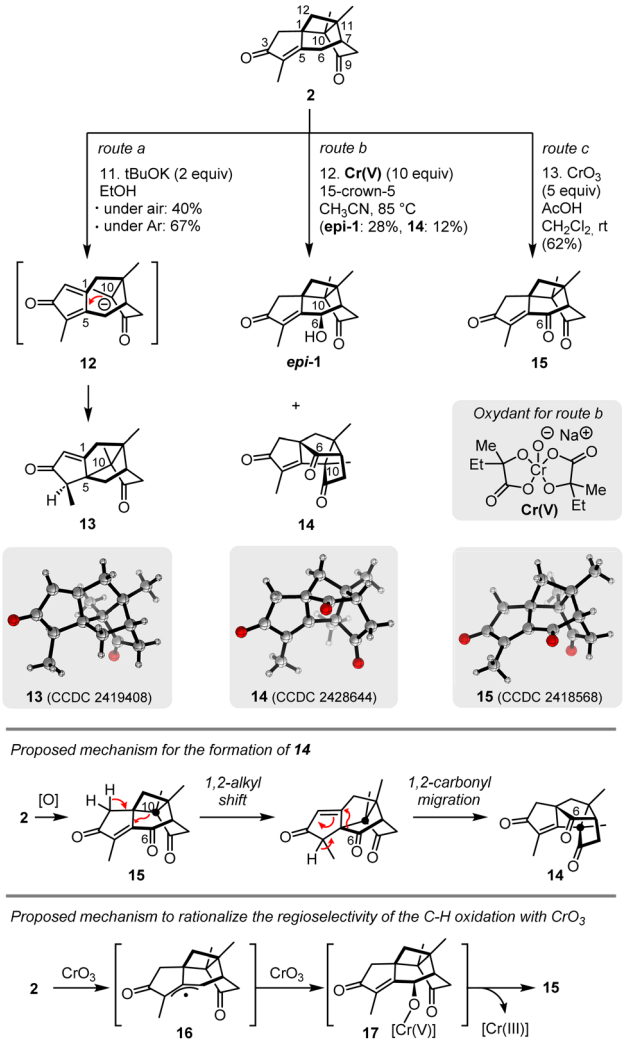

Scheme 4 Late-stage functionalization of **2**. Note: ORTEP structures at 50% probability level (CCDC numbers for **13**: 2419408; **14**: 2428644; **15**: 2418568).‡

directly hydroxylate position C-6, this result also highlighted the unfavourable stereoselectivity of the α-hydroxylation to reach **1**, explained by the higher steric hindrance of the α face. The surprising structure of triketone **14**, confirmed by X-ray crystallography (CCDC 2428644), was supposed to result from a complex rearrangement mechanism (Scheme 4) involving the 1,2-shift of C-10 (similar to that leading to **13**), followed by the 1,2-carbonyl shift of C-6. This proposition is however highly speculative since radical intermediates could also be generated in presence of Cr(v) reagents.

Gratifyingly, oxidation attempts in presence of CrO_3 under acidic condition (CH_2Cl_2/AcOH)[8] furnished enedione **15** in 62% yield (see Table S10† for optimisation). The regioselectivity of this transformation, confirmed by X-ray crystallography (CCDC 2418568), was rationalized by the preferred hydrogen abstraction at C-6, leading to the formation of stabilized radical intermediate **16** (Scheme 4). Reaction of **16** with CrO_3 could form the C–O bond and a Cr(v) species (**17**), while decomposition of **17** would release ketone **15** and Cr(III).[17,54]

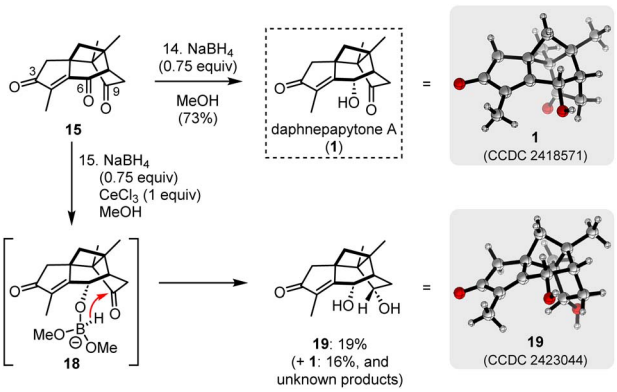

Scheme 5 Final reduction to daphnepapytone A. Note: ORTEP structure at 50% probability level (CCDC numbers for **1**: 2418571; **19**: 2423044).‡

Compound **15** harbours three ketones, two of them embedded in an enedione motif. This structure brought a new challenge for the chemo- and stereoselective reduction of the newly installed ketone on C-6, which was initially overestimated by the apparent accessibility of the cyclopentenone carbonyl on C-3. In fact, this reduction turned out to target exclusively the cyclohexanone ring at C-6, in presence of $NaBH_4$ (0.75 equiv.) in MeOH, delivering daphnepapytone A (**1**) in a 73% yield (Scheme 5) and thus achieving the total synthesis of this natural product. All spectroscopic data of **1** were consistent with those of the literature (Table S11†),[20] including crystallographic analysis (CCDC 2418571). The Luche conditions ($CeCl_3$, $NaBH_4$,

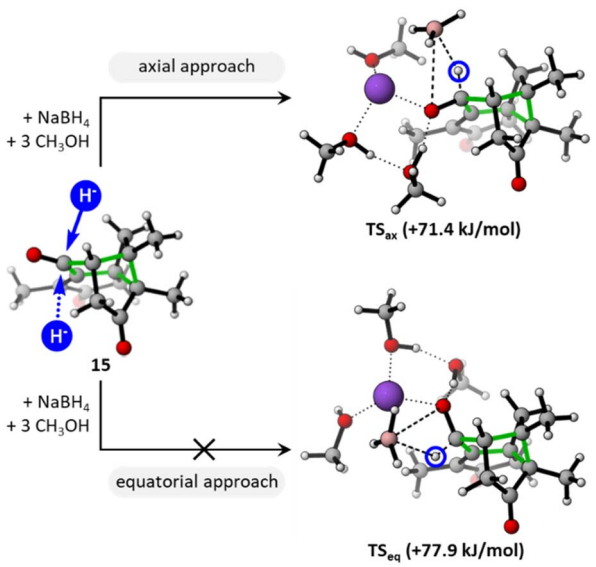

Fig. 2 DFT-supported rationalization of the stereoselectivity observed during the reduction of **15**, favouring an axial approach of the reducing agent (pink: B; purple: Na) onto the cyclohexanone ring (green). DFT approach based on Tomoda's work, considering three explicit solvent molecules (the free energies of transitions states TS_{ax} and TS_{eq} are given relatively to the separated reactants).[59] Calculations performed at the SMD(methanol)-M06-2X/aug-cc-pVTZ//SMD(methanol)-B3LYP-D3/6-311++G(d,p) level (see ESI† for details).‡

MeOH)[55] resulted in poor chemo- and stereoselectivity, giving a mixture of **1** (16%), diol **19** (19%) and other non-identified products. The relative stereochemistry of diol **19** (CCDC 2423044) was explained by the stereocontrolled reduction of the cyclopentanone ring at C-9, after the reduction of C-6, following a Saksena mechanism through boron hydride complex **18**.[56]

Despite an apparent steric hindrance of the ketone on C-6, the high chemoselectivity observed after the reduction could be explained by the faster reaction of cyclohexanones over cyclopentanones.[57,58] The exclusive π-facial stereoselectivity was explained by the favoured axial approach of the hydride nucleophile onto the chair cyclohexanone (green cycle, Fig. 2). Furthermore, not only the disfavoured equatorial approach, but also steric hindrance of the other face imposed by the cage structure, are likely to preclude the formation of the C-6 epimer (***epi*-1** not observed experimentally). DFT calculations confirmed these tendencies. The energy of the transition state TS_{ax} resulting from the axial approach at C-6 (71.4 kJ mol^{-1}) is the lowest among all possible transition states calculated for the reduction of each carbonyl of **1**. In particular, it is lower than TS_{eq} resulting from the equatorial approach (77.9 kJ mol^{-1}). The reduction of the carbonyl groups at C-3 or C-9, within five-membered rings, proves to be more energetic, with activation barriers ranging from 92.8 to 101.3 kJ mol^{-1} (Fig. S5†).

Conclusions

This work represents the first biomimetic total synthesis of daphnepapytone A (**1**). Noteworthily, it was concurrently disclosed at the same time as a non-biomimetic approach by Stoltz.[31,32] We employed a straightforward and highly efficient two-phase strategy, involving a Pauson–Khand reaction to construct the guaiane skeleton, and a biomimetic [2 + 2] cycloaddition to achieve the bridged structure of the target natural product. Remarkably, the late-stage C–H oxidation step was performed in a highly chemoselective manner, resulting in triketone intermediate **15**. The newly installed ketone, the only one localized in a cyclohexanone ring, was chemo- and stereoselectively reduced through an axial approach of the hydride, to release natural product **1**. During this work, peculiar rearrangements of the bridged skeleton were observed, highlighting its reactivity and the possibility to discover new natural product skeletons with similar structures in the near future. Furthermore, three other guaiane products with medicinally relevant properties were synthesized: oleodaphnone (**3**), diarthroncha C (**10**, structure initially reported for the natural product), and daphnenicillata W (**11**). On this occasion, we revised the structure of diarthroncha C, showing that it is the same as daphnenicillata W (**11**). Overall, this work brings a rapid access to the complex caged structure of a structurally unique natural product (**1**) and its biomimetic precursor (**3**) with biological perspectives towards anti-diabetes or anti-HIV treatments.

Data availability

The data supporting this article have been included as part of the ESI.†

Author contributions

B. N. and J. P. designed the synthetic strategy. J. P. performed synthetic experiments. N. C. performed crystallographic analyses. G. F. performed DFT calculations. B. N. supervised the research project and wrote the manuscript. J. P. and G. F. contributed to the discussion.

Conflicts of interest

There are no conflicts to declare.

Acknowledgements

We are grateful to the Ecole Polytechnique, the Centre National de la Recherche Scientifique and the Agence Nationale de la Recherche (ANR-22-CE44-0006) for financial support. We acknowledge ResoMag facility (IP-Paris/CNRS) for the support with NMR facility. We thank Julian Quévarec for his technical support to the Eschenmoser–Tanabe fragmentation.

Notes and references

1 G. Komppa, *Ber. Dtsch. Chem. Ges.*, 1903, **36**, 4332–4335.
2 E. J. Corey, M. Ohno, R. B. Mitra and P. A. Vatakencherry, *J. Am. Chem. Soc.*, 1964, **86**, 478–485.
3 W. Oppolzer and T. Godel, *J. Am. Chem. Soc.*, 1978, **100**, 2583–2584.
4 R. Lavernhe, P. Domke, Q. Wang and J. Zhu, *J. Am. Chem. Soc.*, 2023, **145**, 24408–24415.
5 Y. Yang, D. Xie, L. Huo, Y. Liu, J. Duan, H. Li, P.-P. Zhou, X. Xie and X. She, *Nat. Commun.*, 2025, **16**, 322.
6 K. Chen and P. S. Baran, *Nature*, 2009, **459**, 824–828.
7 R. Marín-Barrios, A. L. García-Cabeza, F. J. Moreno-Dorado, F. M. Guerra and G. M. Massanet, *J. Org. Chem.*, 2014, **79**, 6501–6509.
8 Z. Yuan, X. Hu, H. Zhang, L. Liu, P. Chen, M. He, X. Xie, X. Wang and X. She, *Chem. Commun.*, 2018, **54**, 912–915.
9 Y. Kuroda, K. J. Nicacio, I. A. da Silva-Jr, P. R. Leger, S. Chang, J. R. Gubiani, V. M. Deflon, N. Nagashima, A. Rode, K. Blackford, A. G. Ferreira, L. D. Sette, D. E. Williams, R. J. Andersen, S. Jancar, R. G. S. Berlinck and R. Sarpong, *Nat. Chem.*, 2018, **10**, 938–945.
10 X. Hu, A. J. Musacchio, X. Shen, Y. Tao and T. J. Maimone, *J. Am. Chem. Soc.*, 2019, **141**, 14904–14915.
11 L. A. Wein, K. Wurst, P. Angyal, L. Weisheit and T. Magauer, *J. Am. Chem. Soc.*, 2019, **141**, 19589–19593.
12 M. Berger, C. Knittl-Frank, S. Bauer, G. Winter and N. Maulide, *Chem*, 2020, **6**, 1183–1189.
13 L. A. Wein, K. Wurst and T. Magauer, *Angew. Chem., Int. Ed.*, 2022, **61**, e202113829.
14 Y. Qiu and S. Gao, *Nat. Prod. Rep.*, 2016, **33**, 562–581.
15 I. Bakanas, R. F. Lusi, S. Wiesler, J. Hayward Cooke and R. Sarpong, *Nat. Rev. Chem.*, 2023, **7**, 783–799.
16 Y. Ishihara and P. S. Baran, *Synlett*, 2010, **2010**, 1733–1745.
17 N. C. Wilde, M. Isomura, A. Mendoza and P. S. Baran, *J. Am. Chem. Soc.*, 2014, **136**, 4909–4912.

18 H. Chu, J. M. Smith, J. Felding and P. S. Baran, *ACS Cent. Sci.*, 2017, **3**, 47–51.
19 Y. Kanda, H. Nakamura, S. Umemiya, R. K. Puthukanoori, V. R. Murthy Appala, G. K. Gaddamanugu, B. R. Paraselli and P. S. Baran, *J. Am. Chem. Soc.*, 2020, **142**, 10526–10533.
20 S.-Z. Huang, Q. Wang, J.-Z. Yuan, C.-H. Cai, H. Wang, A. Mándi, T. Kurtán, H.-F. Dai and Y.-X. Zhao, *J. Nat. Prod.*, 2022, **85**, 3–14.
21 M. C. de la Torre and M. A. Sierra, *Angew. Chem., Int. Ed.*, 2004, **43**, 160–181.
22 *Biomimetic Organic Synthesis (1 & 2)*, ed. E. Poupon and B. Nay, Wiley-VCH Verlag, 2011.
23 M. Razzak and J. K. De Brabander, *Nat. Chem. Biol.*, 2011, **7**, 865–875.
24 R. Bao, H. Zhang and Y. Tang, *Acc. Chem. Res.*, 2021, **54**, 3720–3733.
25 L. Chen, P. Chen and Y. Jia, *Acc. Chem. Res.*, 2024, **57**, 3524–3540.
26 S. Li, X. Wang, Y. Yang, X. Wu and L. Zhang, *Int. J. Mol. Sci.*, 2023, **24**, 7357.
27 S. Kitagaki, F. Inagaki and C. Mukai, *Chem. Soc. Rev.*, 2014, **43**, 2956–2978.
28 E. D. Deihl, F. Haghighi and K. M. Brummond, *Org. Synth.*, 2023, **100**, 29–47.
29 A. Eschenmoser, D. Felix and G. Ohloff, *Helv. Chim. Acta*, 1967, **50**, 708–713.
30 M. Tanabe, D. F. Crowe and R. L. Dehn, *Tetrahedron Lett.*, 1967, **8**, 3943–3946.
31 E. C. Gonzalez, I. d. l. T. Roehl and B. M. Stoltz, *ChemRxiv*, 2025, preprint, DOI: **10.26434/chemrxiv-2025-z55dj**.
32 J. Pereira, N. Casaretto, G. Frison and B. Nay, *ChemRxiv*, 2025, preprint, DOI: **10.26434/chemrxiv-2025-0gds5**.
33 Z. Meng and A. Fürstner, *J. Am. Chem. Soc.*, 2019, **141**, 805–809.
34 M. B. Isaac and T.-H. Chan, *J. Chem. Soc. Chem. Commun.*, 1995, 1003–1004.
35 M. Wang, S. Khan, E. Miliordos and M. Chen, *Adv. Synth. Catal.*, 2018, **360**, 4634–4639.
36 S. D. Friis, A. T. Lindhardt and T. Skrydstrup, *Acc. Chem. Res.*, 2016, **49**, 594–605.
37 P. Halder, K. Mondal, A. Jash and P. Das, *J. Org. Chem.*, 2024, **89**, 9275–9286.
38 K. M. Brummond, H. Chen, K. D. Fisher, A. D. Kerekes, B. Rickards, P. C. Sill and S. J. Geib, *Org. Lett.*, 2002, **4**, 1931–1934.
39 K. M. Brummond and D. Gao, *Org. Lett.*, 2003, **5**, 3491–3494.
40 A. S. Bayden, K. M. Brummond and K. D. Jordan, *Organometallics*, 2006, **25**, 5204–5206.
41 F. Grillet, C. Huang and K. M. Brummond, *Org. Lett.*, 2011, **13**, 6304–6307.
42 B. Wen, J. K. Hexum, J. C. Widen, D. A. Harki and K. M. Brummond, *Org. Lett.*, 2013, **15**, 2644–2647.
43 S. M. Wells and K. M. Brummond, *Tetrahedron Lett.*, 2015, **56**, 3546–3549.
44 C. Mukai, I. Nomura, K. Yamanishi and M. Hanaoka, *Org. Lett.*, 2002, **4**, 1755–1758.
45 C. Mukai, I. Nomura and S. Kitagaki, *J. Org. Chem.*, 2003, **68**, 1376–1385.
46 T. Hirose, N. Miyakoshi and C. Mukai, *J. Org. Chem.*, 2008, **73**, 1061–1066.
47 Y. Hayashi, K. Ogawa, F. Inagaki and C. Mukai, *Org. Biomol. Chem.*, 2012, **10**, 4747–4751.
48 S. N. Gockel and K. L. Hull, *Org. Lett.*, 2015, **17**, 3236–3239.
49 D.-X. Sun, D. Zhao, H.-Y. Wei, X.-L. Ma, L.-L. Shi and J. Zhang, *Molecules*, 2018, **23**, 1383.
50 P. Zhao, B.-S. Xin, S.-Y. Qin, Z.-Y. Li, B. Lin, G.-D. Yao, S.-J. Song and X.-X. Huang, *Org. Chem. Front.*, 2022, **9**, 6213–6222.
51 M. T. Crimmins and T. L. Reinhold, in *Organic Reactions*, John Wiley & Sons, Ltd, 2004, pp. 297–588.
52 G. Ciamician and P. Silber, *Ber. Dtsch. Chem. Ges.*, 1908, **41**, 1928–1935.
53 C.-Y. Zheng and J.-M. Yue, *Nat. Commun.*, 2023, **14**, 2399.
54 P. Mueller and J. Rocek, *J. Am. Chem. Soc.*, 1974, **96**, 2836–2840.
55 A. L. Gemal and J. L. Luche, *J. Am. Chem. Soc.*, 1981, **103**, 5454–5459.
56 A. K. Saksena and P. Mangiaracina, *Tetrahedron Lett.*, 1983, **24**, 273–276.
57 H. C. Brown and K. Ichikawa, *Tetrahedron*, 1957, **1**, 221–230.
58 D. E. Ward and C. K. Rhee, *Can. J. Chem.*, 1989, **67**, 1206–1211.
59 Y. Suzuki, D. Kaneno and S. Tomoda, *J. Phys. Chem. A*, 2009, **113**, 2578–2583.